

Supplementary Information

Iron phthalocyanine derived Fe₁/h-BN single atom catalyst for CO₂ hydrogenation

Denis V. Leybo^{1,*}, Anastasia A. Ryzhova¹, Andrei T. Matveev¹, Konstantin L. Firestein², Pavel A. Tarakanov³, Anton S. Konopatsky¹, Alexander L. Trigub⁴, Ekaterina V. Sukhanova⁵, Zakhar I. Popov^{5,6}, Dmitri V. Golberg^{2,7}, and Dmitry V. Shtansky¹

¹ National University of Science and Technology “MISIS”, Leninsky Prospect 4, 119049 Moscow, Russia

² Centre for Materials Science and School of Chemistry and Physics, Faculty of Science, Queensland University of Technology, Brisbane, QLD 4000, Australia

³ Institute of Physiologically Active Compounds at Federal Research Center of Problems of Chemical Physics and Medicinal Chemistry, Russian Academy of Sciences, 1 Severny Proezd, 142432 Chernogolovka, Russia

⁴ National Research Center Kurchatov Institute, 123182, Moscow, Russia

⁵ Emanuel Institute of Biochemical Physics RAS, 199334, Moscow, Russia

⁶ Plekhanov Russian University of Economics, 36 Stremyanny per., 117997, Moscow, Russia

⁷ Research Centre for Materials Nanoarchitectonics, National Institute for Materials Science (NIMS), Namiki 1, Tsukuba, Ibaraki 305, Japan

* Corresponding author, leybo.dv@misis.ru, +74956384415

Tables

Table S1. Comparison of total metal content based mole-specific activity among different catalysts in the literature

Catalyst	Temperature, °C	H ₂ /CO ₂ ratio	Major product	Activity, mol _{CO2} ·mol _{Me} ⁻¹ ·h ⁻¹	Ref.
Single-atom catalysts					
Pt ₁ -MoO _x /Mo ₂ N	200	69/23	CO	3667	1
Ru ₁ /Ni/CeO ₂	225	4	CH ₄	38.6	2
Ir ₁ /TiO ₂	300	1	CO	63.7	3
Pt ₁ /CeO ₂	200	12.5	CO	895	4
Ni ₁ /MgO	250	4	CO	2.94E-02	5
Pt ₁ /Ni/Al ₂ O ₃	250	4	CH ₄	2.66	6
Co ₁ /SBA-15	200	1	CO	9.39E-02	7
Fe ₁ -ox/ <i>h</i> -BN	200	2	CO	44	this work
Fe NPs-based catalysts					
CuFeO ₂	320	3	Olefins	5.21E-01	8
Fe ₂ O ₃ @KO ₂	375	3	C ₂ -C ₄	3.81	9
Na-Fe ₃ O ₄ /HZSM-5	320	2	C ₅ -C ₁₁	2.43	10
Fe/C-Bio	320	3	C ₄ -C ₁₈	2.92	11
Fe _{0.45} Cu _{0.45} K _{0.1} /SAPO-34	300	4	C ₂ -C ₄	5.80E-01	12

Table S2. Sorption energy values of single Fe atoms on the pristine and defected *h*-BN surface calculated via DFT

System	Fe atom position	Sorption energy, eV
pristine <i>h</i> -BN	Above B ₃ N ₃ ring	4.47
	Above B atom	4.26
	Above N atom	4.42
	Above BN bond center	4.38
<i>h</i> -BN with B vacancy	Above vacancy	-3.57
	In vacancy site	-1.92
<i>h</i> -BN with N vacancy	Above vacancy	0.56
	In vacancy site	4.25
<i>h</i> -BN with O substitution	Above O atom	2.16
	Above B closest to O	2.33
	Above B far from O	2.73
	Above BO bond	2.12
<i>h</i> -BN with B vacancy and O atom substitution	Above vacancy	-1.29
	In vacancy site	0.24

Table S3. Sorption energy values of FePc molecules on the pristine and defected *h*-BN surface calculated via DFT

System	Fe atom of FePc molecule position	Sorption energy, eV
pristine <i>h</i> -BN	Above N atom	-2.12
<i>h</i> -BN with B vacancy	Above vacancy	-3.22
<i>h</i> -BN with N vacancy	Above vacancy	-3.06
<i>h</i> -BN with O substitution	Above O atom	-4.18

Table S4. FePc adsorption parameters calculated using different models

Model	Parameter	Value
Langmuir	A_m	238
	b	4.26×10^{-2}
	R^2	0.8696
Freundlich	K_F	66.4
	n	5.27
	R^2	0.3424
Temkin	K_T	22.1
	b_T	20.8
	R^2	0.4828

Figures

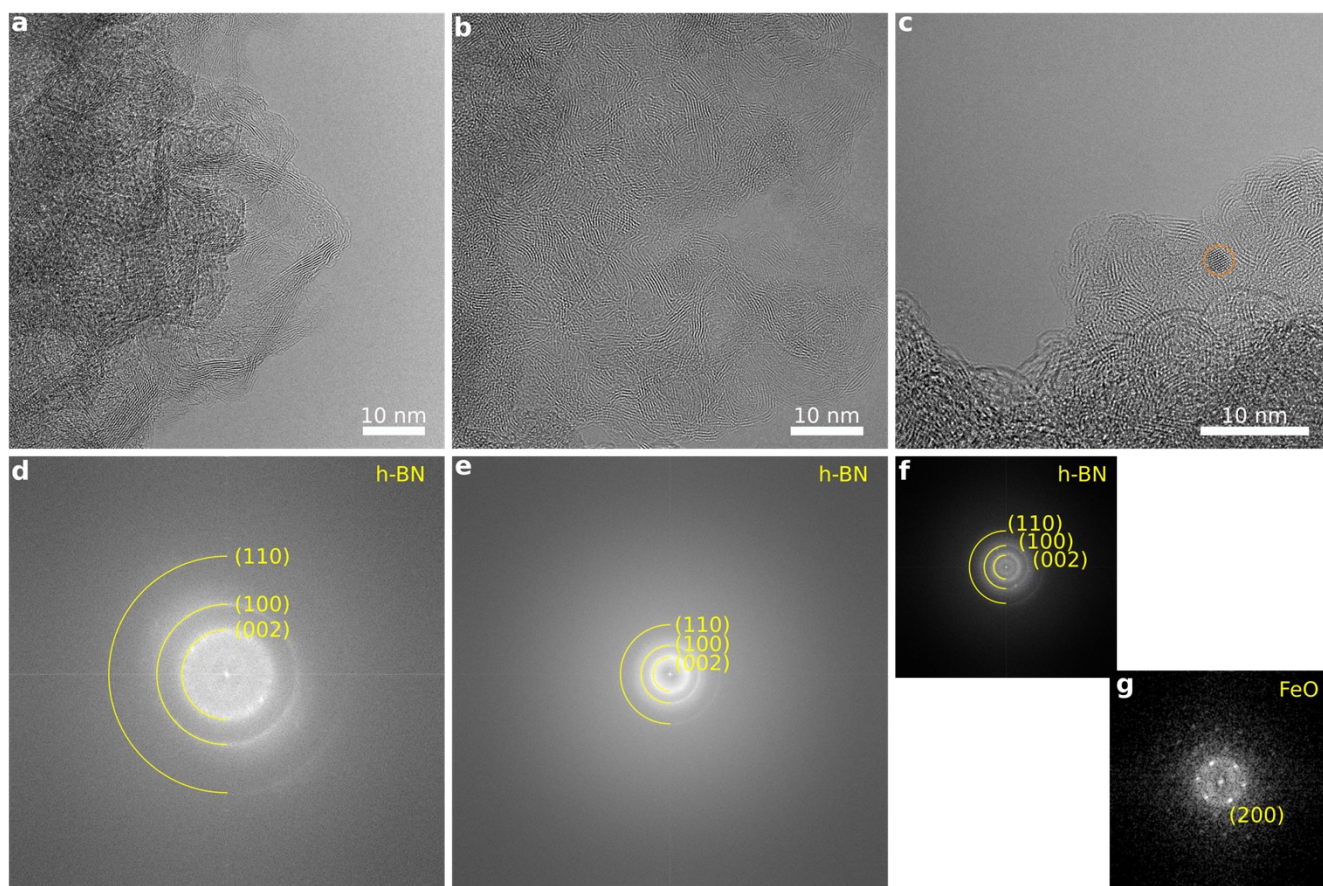


Figure S1. HRTEM (a, b, c) and FFT (d, e, f, g) images of FePc/h-BN (a, d), Fe₁-ox/h-BN (b, e), and Fe₁-red/h-BN (c, f, g) samples. FFT image (g) was obtained from area inside orange circle shown in (c).

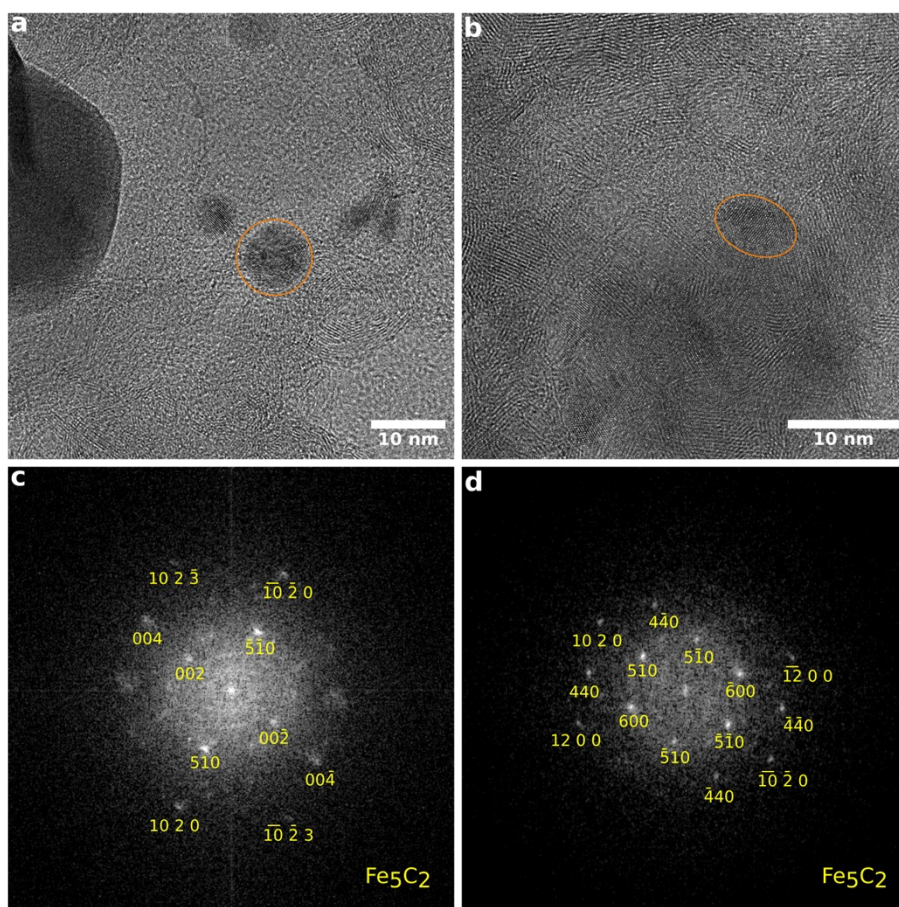


Figure S2. HRTEM (a, b) and FFT (c, d) images of Fe₁-ox/*h*-BN (a, c) and Fe₁-red/*h*-BN (b, d) samples after catalytic experiment. FFT images were obtained from area inside orange circles of corresponding HRTEM images.

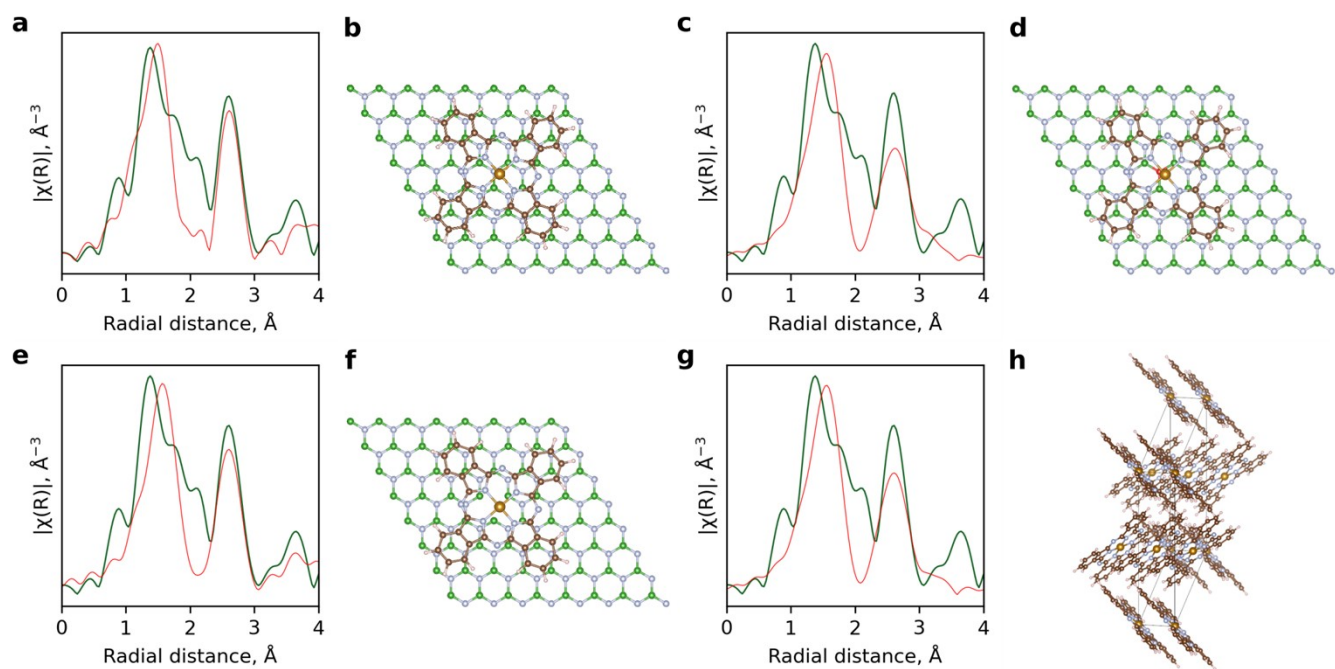


Figure S3. EXAFS spectra fitting (a, c, e, g) using the corresponding structures (b, d, f, h) for FePc/*h*-BN sample: FePc over *h*-BN (b), FePc over O substitution (d), FePc over N vacancy (f), and crystalline FePc (h).

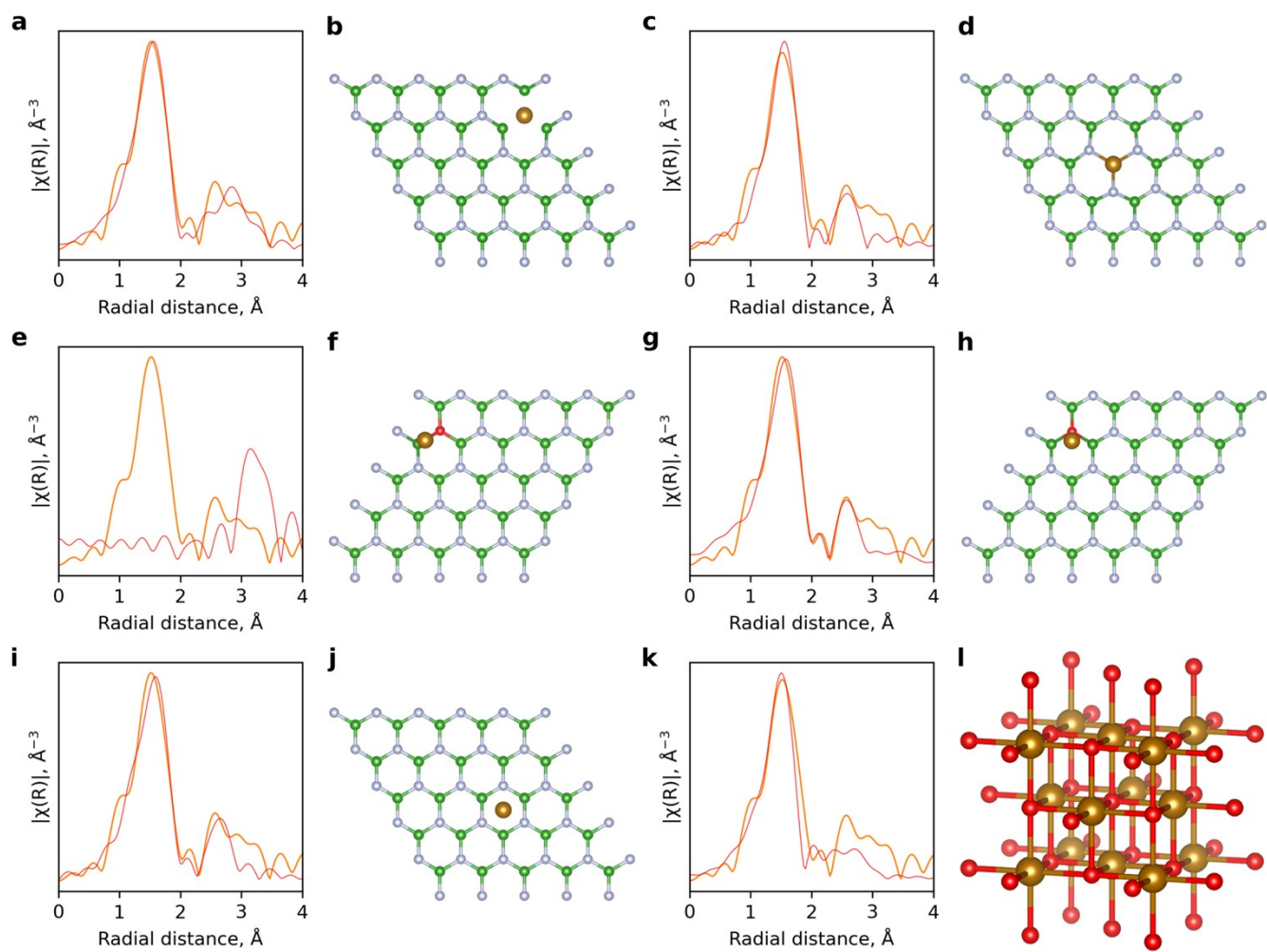


Figure S4. EXAFS spectra fitting (a, c, e, g, i, k) using the corresponding structures (b, d, f, h, j, l) for Fe₁-ox/*h*-BN sample: Fe above N vacancy (b), Fe above B vacancy (d), Fe above BO bond near O substitution (f), Fe above O substitution (h), Fe above BN ring (j), and crystalline FeO (l).

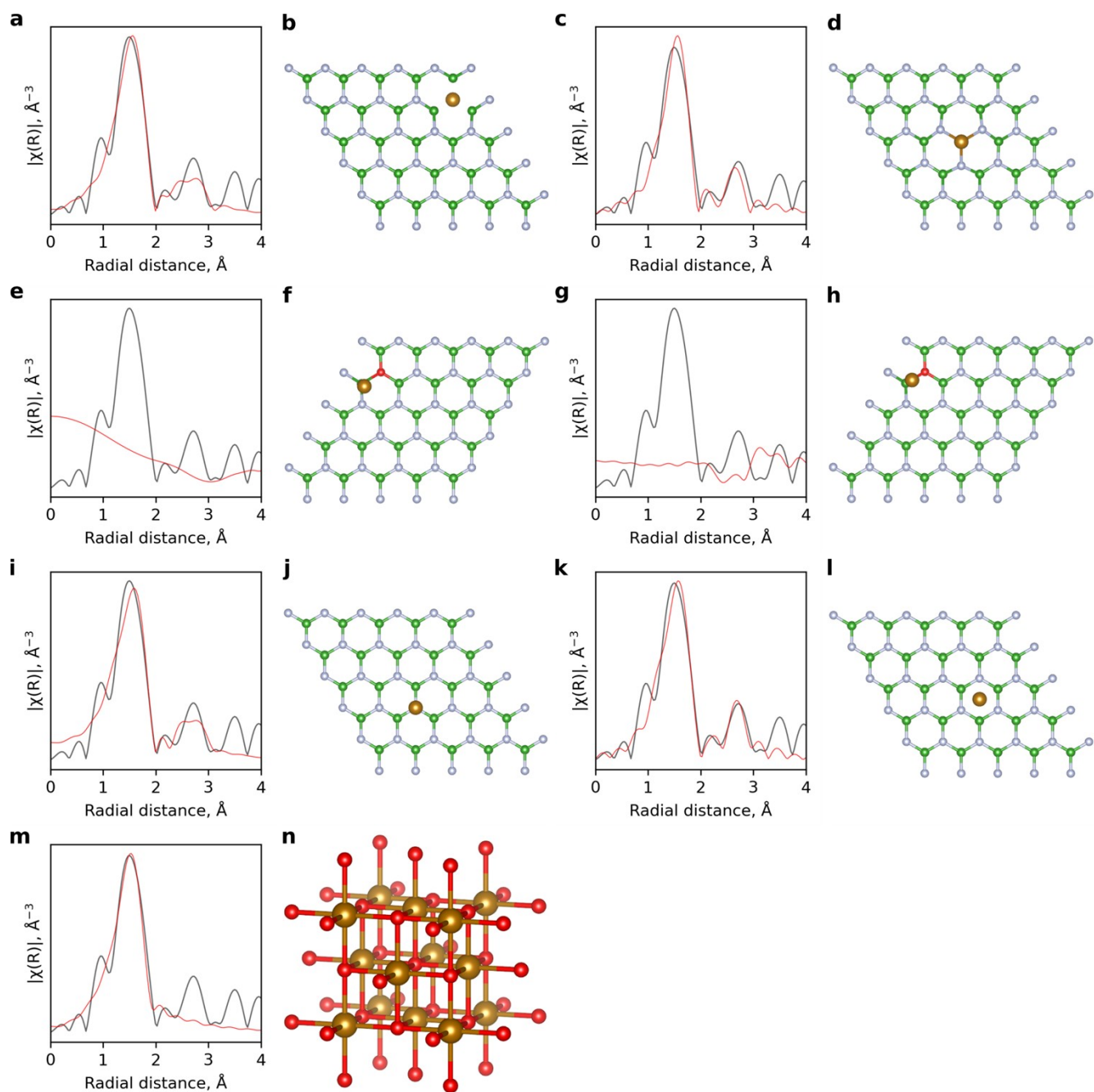


Figure S5. EXAFS spectra fitting (a, c, e, g, i, k, m) using the corresponding structures (b, d, f, h, j, l, n) for Fe₁-red/h-BN sample: Fe above N vacancy (b), Fe above B vacancy (d), Fe above B near O substitution (f), Fe above BO bond near O substitution (h), Fe above N (j), Fe above BN ring (l), and crystalline FeO (n).

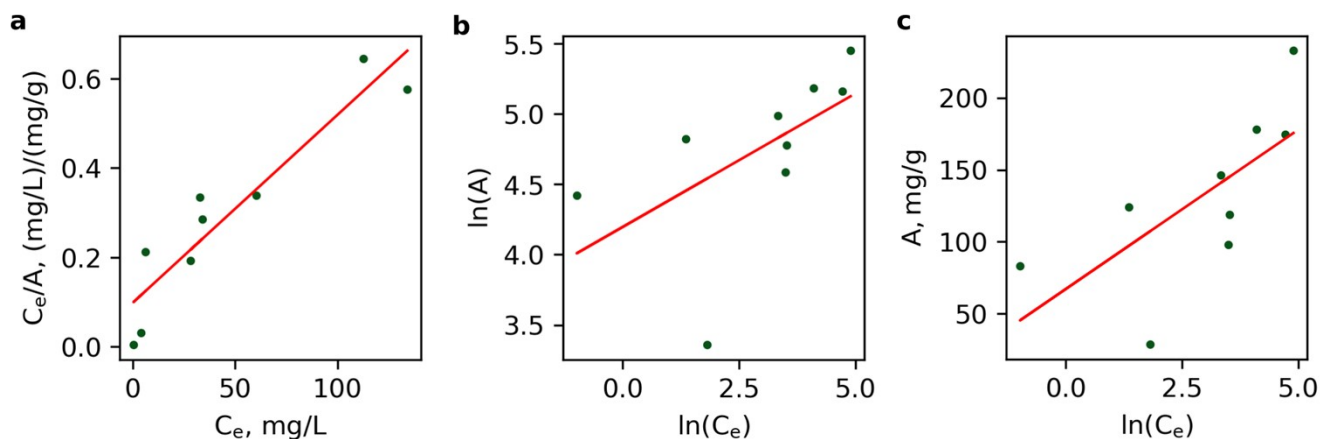


Figure S6. FePc on *h*-BN adsorption isotherms fitting results using Langmuir (a), Freundlich (b), and Temkin (c) adsorption models

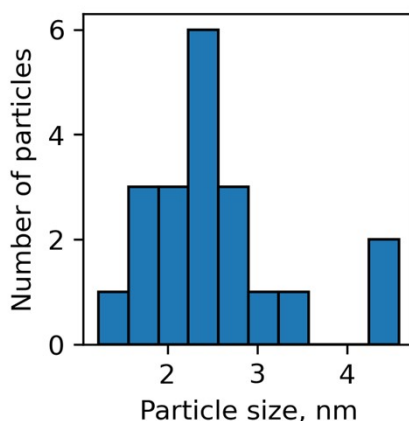


Figure S7. Particle size distribution for Fe₁-red/*h*-BN sample. The histogram was obtained by analysis of 100 HAADF STEM and HRTEM images with total area of 460x460 nm²

DFT calculation details

In order to investigate the coordination environment of single Fe atoms and FePc molecules on *h*-BN, O-doped *h*-BN and *h*-BN with N and B vacancies, the adsorption energies were calculated within DFT as:

$$E_{ads} = E_{ML+ad} - E_{ML} - E_{ad}$$

where E_{ML+ad} is the total energy of the system with the adsorbent (single Fe atom or FePc molecule), E_{ML} is the energy of the adsorbent monolayer (pristine or *h*-BN with defects), and E_{ad} is the energy of adsorbed species – the calculated chemical potential of Fe atom in BCC Fe crystal, or the energy of an isolated FePc molecule.

The calculated sorption energy of an individual FePc molecule on pristine *h*-BN is -2.12 eV. In the case of sorption over a vacancy site, the energy is -3.06 and -3.22 eV for nitrogen and boron monovacancies, respectively, and in the case of oxygen-substituted nitrogen, the adsorption energy is maximum and equal to -4.18 eV, which indicates that the molecule would preferably be anchored over the oxygen atom on the *h*-BN surface.

The calculated adsorption energy of a single Fe atom (FeSA) on the pristine *h*-BN surface is 4.26 eV. In the case of sorption of a FeSA over a defect site, the adsorption energy becomes more negative. One of the most common defects in the *h*-BN structure is monovacancy. In the case of B and N monovacancies, the adsorption energies are -3.57 eV and 0.56 eV, respectively. In both cases, the most energetically favorable position corresponds to the sorption of FeSA above a monovacancy. Another possible defect type is the oxygen-substituted nitrogen in the *h*-BN structure ¹³, which can also take place in our system due to heat treatment in an oxygen atmosphere. For this case, we considered the *h*-BN monolayer, in which one nitrogen atom is replaced by an oxygen atom, as well as *h*-BN monolayer with B vacancy with one nitrogen atom replaced by an oxygen atom. It was found that the most energetically favorable site for sorption of a FeSA is the position above the B vacancy with O-substituted N, with the E_{ads} equal to -1.29 eV. Thus, the most preferable anchoring position for FeSA is determined by the following sequence: B vacancy in *h*-BN < B vacancy with O substituted N atom in *h*-BN < pristine *h*-BN, with corresponding sorption energies of -3.57 < -1.29 < 4.26 eV, respectively. Positive values of sorption energies indicate the thermodynamic advantage of iron cluster agglomeration compared to the existence of FeSA on the *h*-BN surface, which means that these atoms can freely diffuse over the sorbent surface, for example, upon heating.

Comparison of different FePc adsorption models

FePc was deposited onto *h*-BN surface via adsorption from DMF solution in this work. The process of adsorption was studied in more detail by constructing adsorption isotherm at 22±2°C. The amount of FePc adsorbed on *h*-BN was obtained by measurement of Fe content using ICP AES. The equilibrium FePc concentration in the DMF solution was calculated as difference between initial FePc concentration and the amount of adsorbed compound. The adsorption isotherms were compared to Langmuir, Freundlich and Temkin adsorption models. The following equations were used for Langmuir ¹⁴:

$$\frac{C_e}{A} = \frac{C_e}{A_m} + \frac{1}{A_m \cdot b}$$

Freundlich ¹⁴:

$$\ln(A) = \ln(K_F) + \frac{1}{n} \ln(C_e)$$

and Temkin¹⁴ models:

$$A = K_T \ln(b_T) + K_T \ln(C_e)$$

As can be seen from Fig. S6 and Table S4, the data is best approximated by Langmuir equation with highest coefficient of determination (R^2).

Estimation of the mean distance Fe single atoms move to form iron oxide nanoparticle

In order to estimate the mean distance Fe atoms can travel on the surface of *h*-BN during H₂ heat treatment to form 3 nm FeO particle, as in Fig. 5c, we firstly calculated number of Fe atoms needed to form the particle. Using the assumption that the particle is semi-spherical, the number of atoms can be calculated using the equations:

$$N_{Fe} = N_{FeO} = \frac{\rho_{FeO} \cdot V_{FeO} \cdot N_A}{M_{FeO}}$$

$$V_{FeO} = \frac{1}{2} \cdot \frac{4}{3} \cdot \pi \cdot r^3$$

where ρ_{FeO} – density of FeO, g/cm³; V_{FeO} – volume of semi-spherical particle; N_A – Avogadro number; M_{FeO} – FeO molar mass; r – radius of semi-spherical particle.

In this way we calculated that 135 Fe atoms is needed to form semi-spherical FeO particle 3 nm in diameter.

In the next step we assumed that 135 Fe atoms are uniformly distributed on the surface of *h*-BN, forming 2D square lattice, with surface density of 13 atoms / 100 nm², as was estimated from HAADF STEM images of Fe₁-ox/*h*-BN sample. The distance between adjacent Fe atoms can be calculated using the equation:

$$a = \sqrt{\frac{1}{d_s}}$$

Average distance Fe atoms move to form particle was estimated as an average distance from each Fe atom of the square lattice to the center atom of the lattice. The distances were calculated numerically using following code, written in Python programming language (see illustration to the code below):

```
import numpy as np
```

```

def calculate_average_distance(N:int, a:float) -> float:
    """
        Calculate average distance between central atom with coordinate (0,0) and
        N-1 atoms with coordinates (x,y) forming 2D square lattice with distance between
        adjacent atoms equal to a.
    """
    def measure_dist(x:int, y:int) -> float:
        """
            Calculate distance between atom with coordinate (x,y) and central atom
            with coordinate (0,0)
        """
        d = a * np.sqrt(x**2 + y**2)
        return d
    distances = [] # list of distances between atoms with central atom
    ct = 1 # counter which counts how much atoms were encountered so far
    while True:
        sq = 1 # calculate distances from atoms in the first square around the
        central atom
        # take each atom with coordinate (x,y), where -sq >= x,y >= sq
        # calculate distance from the atom to the central atom with coordinate
        (0,0) and append the result to the list of distances
        # if there are N atoms in the list, calculate and return mean distance
        y = sq
        for x in range(-sq, sq+1, 1):
            d = measure_dist(x, y)
            distances.append(d)
            ct += 1
            if ct == N:
                d_av = np.mean(distances)
                return float(d_av)
        x = sq
        for y in range(-sq, sq+1, 1):
            if y != sq:
                d = measure_dist(x, y)
                distances.append(d)
                ct += 1
                if ct == N:
                    d_av = np.mean(distances)
                    return float(d_av)
        y = -sq

```

```

for x in range(-sq, sq+1, 1):
    if x != sq:
        d = measure_dist(x, y)
        ct += 1
    if ct == N:
        d_av = np.mean(distances)
        return float(d_av)
x = -sq
for y in range(-sq, sq+1, 1):
    if y != -sq and y != sq:
        d = measure_dist(x, y)
        ct += 1
    if ct == N:
        d_av = np.mean(distances)
        return float(d_av)
sq += 1 # proceed to the next square around the central atom

```

```

if __name__ == '__main__':
    d = calculate_average_distance(135, np.sqrt(100/13)) # calculate average
distance for 2D square lattice of 135 atoms with distance between adjacent atoms
equal to square root of 100/13 (reciprocal of surface density)
print(f'average distance = {d} nm')

```

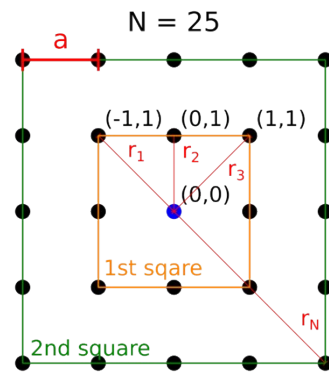


Illustration of 2D square lattice with 25 atoms and main parameters used by the program to calculate average distance to the central atom.

References

- 1 H.-X. Liu, J.-Y. Li, X. Qin, C. Ma, W.-W. Wang, K. Xu, H. Yan, D. Xiao, C.-J. Jia, Q. Fu and D. Ma, *Nature Communications*, 2022, **13**, 5800.
- 2 T. Zhang, P. Zheng, F. Gu, W. Xu, W. Chen, T. Zhu, Y.-F. Han, G. Xu, Z. Zhong and F. Su, *Applied Catalysis B: Environmental*, 2023, **323**, 122190.
- 3 X. Chen, X. Su, H.-Y. Su, X. Liu, S. Miao, Y. Zhao, K. Sun, Y. Huang and T. Zhang, *ACS Catal.*, 2017, **7**, 4613–4620.
- 4 Y. Wang, H. Arandiyana, J. Scott, K.-F. Aguey-Zinsou and R. Amal, *ACS Appl. Energy Mater.*, 2018, **1**, 6781–6789.
- 5 M.-M. Millet, G. Algara-Siller, S. Wrabetz, A. Mazheika, F. Girgsdies, D. Teschner, F. Seitz, A. Tarasov, S. V. Levchenko, R. Schlögl and E. Frei, *J. Am. Chem. Soc.*, 2019, **141**, 2451–2461.
- 6 S. Kikkawa, K. Teramura, H. Asakura, S. Hosokawa and T. Tanaka, *J. Phys. Chem. C*, 2019, **123**, 23446–23454.
- 7 H. Liang, B. Zhang, P. Gao, X. Yu, X. Liu, X. Yang, H. Wu, L. Zhai, S. Zhao, G. Wang, A. P. van Bavel and Y. Qin, *Chem Catalysis*, 2022, **2**, 610–621.
- 8 Z. Li, W. Wu, M. Wang, Y. Wang, X. Ma, L. Luo, Y. Chen, K. Fan, Y. Pan, H. Li and J. Zeng, *Nature Communications*, 2022, **13**, 2396.
- 9 A. Ramirez, X. Gong, M. Caglayan, S.-A. F. Nastase, E. Abou-Hamad, L. Gevers, L. Cavallo, A. Dutta Chowdhury and J. Gascon, *Nature Communications*, 2021, **12**, 5914.
- 10 J. Wei, Q. Ge, R. Yao, Z. Wen, C. Fang, L. Guo, H. Xu and J. Sun, *Nature Communications*, 2017, **8**, 15174.
- 11 L. Guo, J. Sun, X. Ji, J. Wei, Z. Wen, R. Yao, H. Xu and Q. Ge, *Communications Chemistry*, 2018, **1**, 11.
- 12 J. Ding, Q. Liu, R. Ye, W. Gong, F. Zhang, X. He, Y. Zhang, Q. Zhong, M. D. Argyle and M. Fan, *J. Mater. Chem. A*, 2021, **9**, 21877–21887.
- 13 Q. Weng, D. G. Kvashnin, X. Wang, O. Cretu, Y. Yang, M. Zhou, C. Zhang, D.-M. Tang, P. B. Sorokin, Y. Bando and D. Golberg, *Advanced Materials*, 2017, **29**, 1700695.
- 14 J. M. Thomas and W. J. Thomas, *Principles and Practice of Heterogeneous Catalysis*, VCH, Weinheim, 1997.